ATMOSPHERIC SCIENCE LETTERS
Atmos. Sci. Let. **13**: 180–186 (2012)
Published online 27 April 2012 in Wiley Online Library
(wileyonlinelibrary.com) **DOI:** 10.1002/asl.377

RMetS
Royal Meteorological Society

Large-eddy simulation of urban boundary-layer flows by generating turbulent inflows from mesoscale meteorological simulations

Hiromasa Nakayama,[1]* Tetsuya Takemi[2] and Haruyasu Nagai[1]
[1]*Research Group for Environmental Science, Japan Atomic Energy Agency, Tokai, Ibaraki, Japan*
[2]*Disaster Prevention Research Institute, Kyoto University, Uji, Kyoto, Japan*

**Correspondence to: H. Nakayama, Japan Atomic Energy Agency, 2–4 Shirakatashirane, Tokai, Ibaraki 319-1195, Japan. E-mail: nakayama.hiromasa@jaea.go.jp*

Received: 7 July 2011
Revised: 5 March 2012
Accepted: 5 March 2012

Abstract

We propose an approach to generate turbulent flows by using mesoscale meteorological simulations in order to conduct building-resolving large-eddy simulations (LESs) of boundary-layer flows over urban areas under realistic meteorological conditions. The urban surface geometry was explicitly represented in the LES model. This approach was applied for a strong wind event in Tokyo owing to the landfall of a major typhoon whose intensity and track were well reproduced in the meteorological simulation. The observed ranges of wind fluctuations and gust factors and significant decelerations of wind speeds within the urban canopy layer were successfully represented in the LES. Copyright © 2012 Royal Meteorological Society

Keywords: large-eddy simulation; turbulent generation; urban boundary layer

1. Introduction

The variability of atmospheric flow is induced by meteorological disturbances, terrains, and surface roughness elements. Particularly, for highly rough surface such as urban area, high-rise buildings have significant influences on small-scale fluctuations of atmospheric flow. In cases of strong winds induced by meteorological disturbances, the occurrence of gusty winds over such urban areas will be critical in terms of disaster prevention and urban planning.

For understanding the wind system over urban areas a numerical modeling is a useful tool. To simulate atmospheric flows in real meteorological settings, numerical weather prediction (NWP) models are commonly used. Although the accuracy of NWP models for daily weather is continuously improving, it is difficult to reproduce wind fluctuations due to the effects of urban buildings that are not explicitly represented in NWP models.

For simulating wind flows over various arrangements of urban roughness obstacles, a computational fluid dynamics (CFD) technique is commonly used. In CFD models, urban surface geometries can be explicitly represented at high resolutions. In particular, the CFD simulations using large-eddy simulation (LES) are effective to simulate not only boundary-layer structures but also turbulent natures of wind fluctuations within and over roughness obstacles. Therefore, an approach to couple the LES-based CFD and the NWP model should be promising to simulate turbulent winds over actual urban areas under real meteorological conditions. For example, Xie (2011) emphasized the importance of incorporating meteorological effects into CFD models by coupling NWP and CFD models.

In order to couple NWP and CFD models, the NWP outputs can be used as the initial and boundary conditions of a CFD model. Here, a serious issue is encountered when imposing time-dependent turbulent inflow data for LESs from the NWP outputs, because the NWP models are not able to reproduce high-frequency turbulent fluctuations appropriate to drive LES models. Therefore, a proper technique to generate turbulent flows for LESs is required. Golaz *et al*. (2009) used periodic conditions at the four lateral boundaries in order to generate turbulent flows over a flat surface and ingested these turbulent flows into the analysis domain with terrains by a one-way nesting technique. This approach using periodic boundary conditions is effective only when surface geometry is homogeneous. However, the periodic conditions are clearly inappropriate for densely built urban areas where surface geometry is highly inhomogeneous.

To effectively generate turbulent inflows without using a simple periodic boundary condition, the recycling method of Lund *et al*. (1998) is useful. They set a special domain to generate turbulence by rescaling the velocity field at a downstream station and reintroducing at the inlet within the special domain; this turbulent inflow is used for the inputs for a main domain with urban surfaces. Kataoka and Mizuno (2002) and Mayor *et al*. (2002) simplified the method of Lund *et al*. (1998); their approaches are to recycle only the fluctuating components from the averaged winds at a downstream station and add the fluctuations to the mean winds at the inlet. This idea seems to be appropriate in imposing the inflow boundary of the CFD

model from the NWP outputs, because the structure of mean flow is maintained and unaffected by the fluctuations; the NWP outputs can be regarded as a mean flow.

In this study, we apply the inflow generation technique of Kataoka and Mizuno (2002) and Mayor *et al*. (2002) to couple the CFD and NWP models. We conduct an LES of strong winds over the central district of Tokyo during the passage of a major typhoon and examine the usefulness of our approach by comparing the simulated results with the observations.

2. Numerical model

2.1. Mesoscale meteorological simulation model

The model used for a mesoscale meteorological simulation is the Weather Research and Forecasting (WRF) model, the Advanced Research WRF Version 3.1.1 (Skamarock *et al*., 2008). We use a nesting capability to resolve the Tokyo region at a fine grid spacing by setting one-way nested, four computational domains (with the top being at the 50 hPa level). The four domains cover areas of 1800 km × 1900 km at 4.5 km grid, 270 km × 300 km at 1.5 km grid, 93 km × 93 km at 300 m grid, and 25 km × 30 km at 60 m grid, respectively (Figure 1(a)–(d)). The number of vertical levels is 43, with 15 levels in the lowest 1 km depth.

The terrain data used are the global 30 s data (GTOPO30) from the US Geological Survey for the outer two domains and the 50 m mesh digital elevation dataset by the Geographical Survey Institute of Japan for the inner two domains. The land-use/land-cover information is obtained from the 100-mesh dataset from the Ministry of Land, Infrastructure, Transport and Tourism of Japan.

To determine the initial and boundary conditions, we use 6 hourly mesoscale analysis (MANAL) data of Japan Meteorological Agency (JMA), 6 hourly final analysis data of the US National Centers for Environmental Prediction, and daily merged sea surface temperature (MGDSST) analyses of JMA. The horizontal resolutions of MANAL and MGDSST are 10 km and 0.25°, respectively.

Full physics processes are included in the present simulation in order to reproduce real meteorological phenomena. A physics parameterization closely relevant to the simulation of wind fields is a planetary boundary layer (PBL) mixing parameterization. We choose a Mellor–Yamada Level 2.5 scheme of Janjic (2002) in which mixing is done vertically between the adjacent vertical levels. A Kain–Fritch cumulus scheme is used only for the outermost domain, and a water and ice phase microphysics scheme is employed for cloud and precipitation processes in all the domains. Note that canopy model for representing urban turbulence effects is not applied here.

The case studied is a high-wind event in Tokyo during the passage of Typhoon Melor (2009) that attained the central pressure of 910 hPa and the maximum 10 min averaged wind of 55 m s^{-1} at its maximum intensity on 4 October 2009 and made landfall on the Japan coast about 280 km west of Tokyo at around

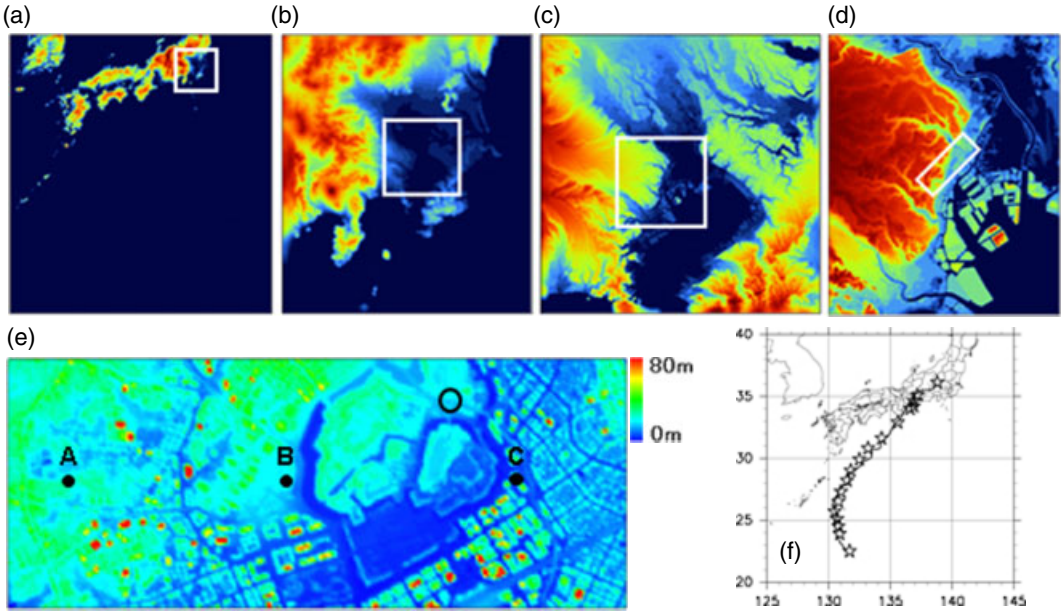

Figure 1. Computational areas of the nested WRF models for (a) the 4.5 km grid, (b) the 1.5 km grid, (c) the 300 m grid, and (d) the 60 m grid domains and of (e) the CFD model. (f) The track of Typhoon Melor (2009). The inflow boundary of the CFD model is on the left. The color shading in (a)–(d) indicates the surface elevation scaled by the maximum height in each domain (2409 m in (a); 3285 m in (b); 255 m in (c); and 54 m in (d)). The white rectangular in (a)–(d) indicates the area of the child domain. The color shading in (e) indicates the height of the buildings and structures. The circle and the points A, B, and C in (e) represent the locations of the wind observation site and the points used in Figure 5, respectively. The black line and the star in (f) indicate the typhoon track of the WRF simulation and the best-track data, respectively.

2000 UTC 7 October. The maximum instantaneous wind speed recorded in Tokyo was 30.2 m s^{-1} at 2339 UTC 7 October. In order to simulate wind fields for this event, the computation for the outermost domain is initialized at 0000 UTC 6 October 2009, while the simulations for the three innermost domains are initialized at 1800 UTC 7 October. The simulated outputs of the innermost domain at 1 min interval are used as the inputs of a CFD model.

2.2. Urban CFD model

The CFD model is based on the LES model developed by Nakayama *et al*. (2011). The buildings in the central district of Tokyo are explicitly represented in the CFD model by the use of a digital surface model dataset at 2 m resolution. In the CFD model, the size of the domain where the urban surface geometry is explicitly resolved is 5.0 km (streamwise) × 2.0 km (spanwise) with the depth of 1.5 km (Figure 1(e)), with buffer zones with a 500 m length being placed at the up- and downstream of the building-resolved area. Thus, the length of the main analysis domain is 6.0 km, which is along the dominant wind direction (i.e. the southwest–northeast). The total mesh number is $300 \times 100 \times 80$ nodes. The grid spacing is 20 m in the horizontal directions and 2.5–64 m stretched in the vertical direction. The packing density of the buildings and the mean and standard deviation of building heights shown in Figure 1(e) are 0.63, 21.2, and 19.2 m, respectively.

The governing equations are the spatially filtered continuity and Navier-Stokes equations. The subgrid turbulence mixing is represented by the standard Smagorinsky model (Smagorinsky, 1963) with the Smagorinsky constant of 0.1. The building effect is represented by an external force formulated by Goldstein *et al*. (1993); wind speeds at grids within buildings are effectively damped and become almost zero. The coupling algorithm of the velocity and pressure fields is based on the marker-and-cell (MAC) method (Chorin, 1967) with the Adams-Bashforth scheme for time integration. The time step is set to 0.05 s in order to avoid numerical instability. The Poisson equation is solved by the successive over-relaxation (SOR) method. For the spatial discretization, a second-order-accurate central difference is used.

The boundary conditions without applying the WRF outputs are: a Sommerfeld radiation condition (Gresho, 1992) at the outflow boundary; a free-slip condition for the horizontal velocity components and zero-speed condition for the vertical velocity component at the upper boundary; a no-slip condition for each velocity component at the bottom surface. At the spanwise boundaries, a periodic condition is imposed. On the other hand, the inflow boundary condition is determined by the WRF model outputs (with 1 min interval and 60 m resolution) linearly interpolated on the temporal and spatial resolutions of LES. It should be mentioned that the spanwise periodic condition cannot accurately reproduce real situations where wind direction actively changes.

2.3. Coupling of WRF and urban CFD models

The WRF model cannot reproduce small-scale wind fluctuations due to urban-like obstacles because individual buildings and structures are not explicitly resolved. To ingest the WRF outputs for a building-resolving LES, turbulent fluctuations due to urban geometry should be added to the WRF outputs. Various methods to generate turbulent inflows for use in LESs have been proposed. As mentioned in Section 1, a type of the recycling approach of Lund *et al*. (1998) is considered to be useful in terms of both saving computational resources and physical consistency to boundary-layer dynamics. A recycling technique of Kataoka and Mizuno (2002) has an advantage in quickly generating turbulent flows with a short fetch by maintaining averaged inflow steady. However, assuming a steady mean flow at the inflow boundary is not appropriate to simulate atmospheric flows under real meteorological conditions because the mean flow actually changes with time owing to the meteorological variations. Therefore, we extend the method of Kataoka and Mizuno by taking into account the temporal and spatial variations of the mean flow at the inflow boundary of the CFD model. These variations are given by the WRF outputs and regarded as a basic flow for the CFD model.

The inlet boundary condition of a special domain intended to drive turbulent flows (i.e. a driver domain) is formulated as follows:

$$u_{\mathrm{inlt}}(y,z,t) = \langle u\rangle_{\mathrm{WRF}}(y,z,t) + \phi(z)\{u_{\mathrm{recy}}(y,z,t) - [u](z)\} \quad (1)$$

$$v_{\mathrm{inlt}}(y,z,t) = \langle v\rangle_{\mathrm{WRF}}(y,z,t) + \phi(z)\{v_{\mathrm{recy}}(y,z,t) - [v](z)\} \quad (2)$$

$$w_{\mathrm{inlt}}(y,z,t) = \langle w\rangle_{\mathrm{WRF}}(y,z,t) + \phi(z)\{w_{\mathrm{recy}}(y,z,t) - [w](z)\} \quad (3)$$

where, u, v, and w are the wind components of the streamwise (x), spanwise (y), and vertical (z) directions, respectively, and the suffixes of inlt and recy indicate the instantaneous wind components at the inlet and the downstream position (i.e. the recycle station), respectively. $\langle u\rangle_{\mathrm{WRF}}$, $\langle v\rangle_{\mathrm{WRF}}$, and $\langle w\rangle_{\mathrm{WRF}}$ are wind components of the WRF model at the inlet location; $[u]$, $[v]$, and $[w]$ are horizontally averaged winds over the driver domain; $\phi(z)$ is a damping function to control the unwanted development of fluctuations in the upper part of the simulated boundary layer. This function applied here is represented by a hyperbolic tangent function, and rapidly damps from 1.0 to 0.0 across 500 m height.

The other boundary conditions of the driver domain are the same as those of the main analysis domain. The size of this driver domain is 1.0 km (streamwise) ×

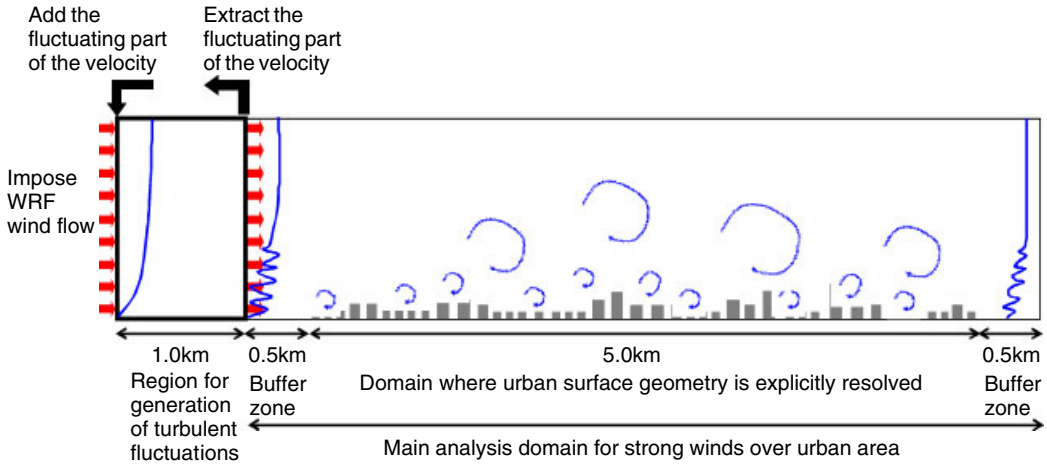

Figure 2. Schematic diagram of the present numerical model for generating turbulent flows.

2.0 km (spanwise) with the depth of 1.5 km. The mesh numbers are 50 (streamwise) by 100 (spanwise) by 80 (vertical) nodes; thus, the grid spacings are the same as those for the main analysis domain.

Figure 2 shows a schematic diagram of the turbulence generation method for the present LES. First, three-dimensional, time-dependent winds obtained from the WRF model are imposed at the inlet boundary of the driver domain, and a basic boundary-layer flow with turbulent fluctuations is generated in the downstream direction. Then, only fluctuation components are extracted at a downstream point, and recycled back to the inlet boundary by adding them to the WRF winds. After recycling, the turbulent inflow with the WRF winds being the basic flow is generated at the outlet of the driver domain; this turbulent inflow is imposed at the upstream boundary of the main analysis domain having realistic urban geometry and adjusted to a rough-wall boundary-layer flow within about 1 km distance from the upstream boundary. The WRF outputs during 2300 UTC 7 October and 0000 UTC 8 October are used for the present LES.

3. Results

The simulated central pressure just before the landfall at around 2000 UTC 7 October was 953 hPa, which well agrees with the corresponding best-track value of 955 hPa. In addition, the observed track of Typhoon Melor (2009) was well reproduced in the outermost domain of the WRF model (Figure 1(f)). Thus, the WRF model is considered to successfully simulate the track and intensity of Typhoon Melor (2009) before and during the landfall on 7 October 2009, which indicates that the WRF outputs for use in the present LES reflect the overall features of the strong winds induced by the typhoon.

After applying the recycling technique described in Section 2.3., turbulence was quickly generated within the driver domain. Figure 3 shows the vertical profiles of the mean wind speed, turbulence kinetic energy, and Reynolds stress at the inlet and the recycle station. It is seen that well-developed turbulent fluctuations are generated and at the same time the structure of mean flow is maintained.

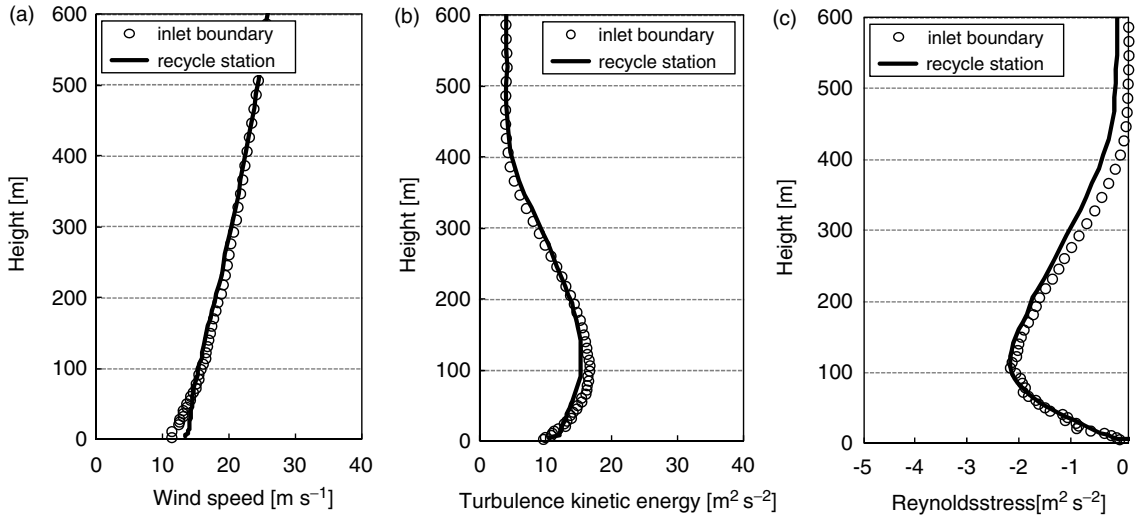

Figure 3. The vertical profiles of turbulence statistics of the generated flow from the WRF outputs at the inlet (circle) and the recycle (solid line) station. (a) Mean wind speed, (b) turbulence kinetic energy, and (c) Reynolds stress.

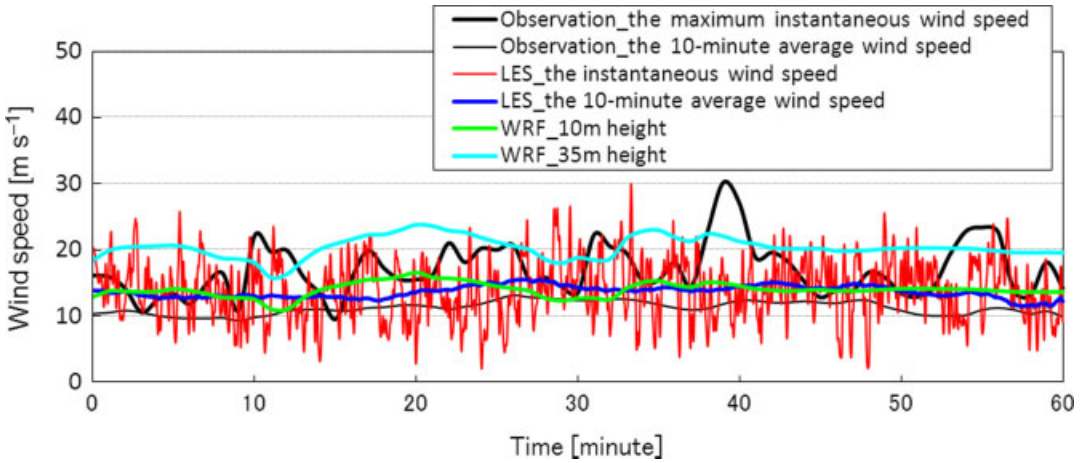

Figure 4. Time series of the horizontal wind speeds of the 10 min means (thin black line) and the maximum instantaneous values (bold black line) at the JMA observation site (the circle point in Figure 1(e)), the WRF simulation obtained at the 10 m height (green line), and the 10 min averaged (blue line) and instantaneous (red line) values from the LES obtained at the 35 m height during the period between 2300 UTC 7 October and 0000 UTC 8 October.

Figure 4 compares the time series of 10 min averaged and instantaneous (in 1 min interval) wind speeds obtained at the JMA observation site (Figure 1(e)) and the simulated wind speed at the corresponding location in the WRF model during 2300 UTC 7 October and 0000 UTC 8 October. The wind observations are conducted at the top of a building and at the 35 m height from the ground surface, while the WRF winds are those at the 10 m height as a representative of the surface winds and the 35 m height. The WRF winds at the 10 m height generally agree well with the observations, but with a slight overestimation. Note that the WRF winds increase with height and those at the 35 m height are about two times stronger than the observed mean winds, suggesting that the WRF model cannot reproduce urban-canopy flows.

The comparison of the LES results with the observation is also shown in Figure 4. The LES winds are those obtained at the 35 m height at the observation location, and their instantaneous values are indicated as 3 s running means. These temporally filtered data are evaluated by taking the moving averages at 3 s interval and plotted at 0.05 s interval. Although the means in the LES slightly overestimate the observed mean winds, the discrepancy between the simulation and the observation is generally within 10%. Furthermore, the instantaneous LES winds seem to vary within the range of the observed maximum instantaneous values.

The streamwise variation of the vertical profiles of wind speeds from the WRF and the LES models are shown in Figure 5. The points A, B, and C are located at 1.0, 2.7, and 4.6 km distances downstream of the upstream boundary of the main analysis domain (Figure 1(e)). The LES winds seem to fluctuate around the WRF winds above about the 100 m height, while the LES winds are significantly weaker than the WRF winds below that level (i.e. urban canopy layer). These deficits in the LES at the lowest levels are obviously due to the blocking effects of buildings that

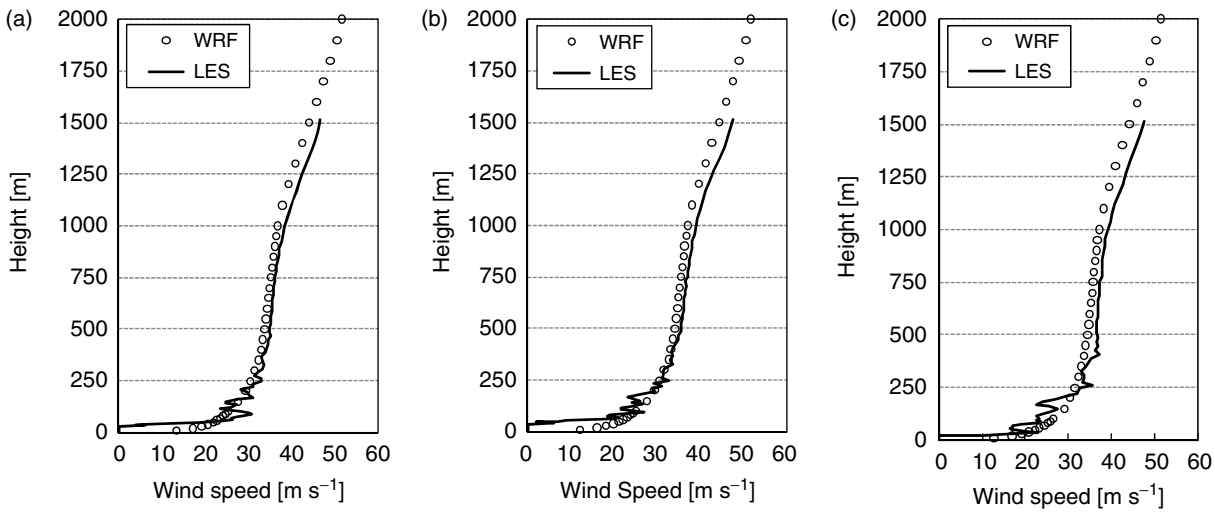

Figure 5. The vertical profiles of wind speeds from the WRF (circles) and the LES (solid line) models at the points (a) A, (b) B, and (c) C (Figure 1(e)) at 0000 UTC 8 October 2009.

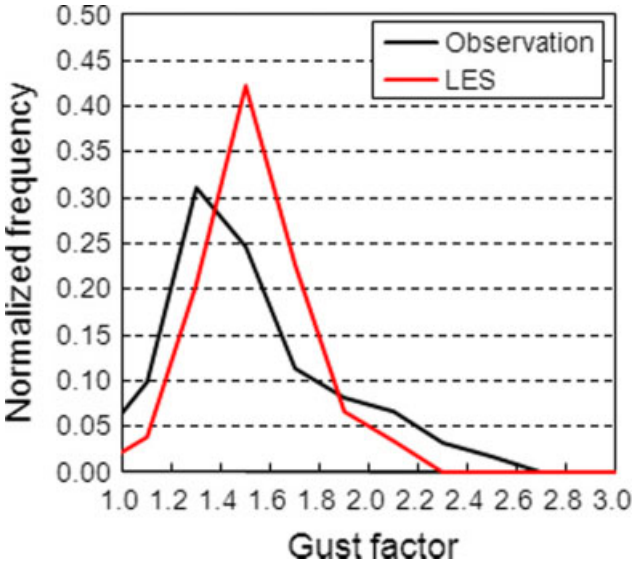

Figure 6. Normalized frequency distribution of gust factors from the observation (black line) and the LES (red line).

are explicitly resolved in the LES. Furthermore, the turbulent fluctuations in the LES are well represented in the streamwise direction, which indicates that the present approach is successful in maintaining turbulence throughout the analysis domain.

In order to evaluate the performance of the LES, we compare gust factors from the LES with the observed values. The gust factor is computed as the ratio of the maximum 3 s running mean wind speeds to the 10 min averaged wind speeds. Figure 6 indicates the frequency distributions of gust factors from the observation and the LES. The frequency distribution obtained from the LES seems to correspond well with that from the observation. There are, however, some differences between the LES and the observation: the representation of the peak frequency and the overestimation (underestimation) of the frequency below (above) the gust factor of 2.0. These differences may be partly due to the result that the fluctuations simulated in the WRF model, in spite of the high-frequency outputs, have smaller variations than those observed (Figure 4); if larger fluctuations, which should be present in real settings, could be simulated in the WRF model, gust factors represented in the LES would be enhanced. A point stressed in this study is that the building effects are a significant contributor in determining the gust factors within the urban canopy.

4. Conclusions

A recycling technique for turbulent inflow generation (Kataoka and Mizuno, 2002) was extended to ingest turbulent flows from NWP simulations into CFD models in order to conduct building-resolving LESs over urban areas under real meteorological conditions. The present approach was used to conduct an LES of urban boundary-layer flows in a real meteorological setting, that is, a strong wind event over the central district of Tokyo during the passage of Typhoon Melor (2009). The urban surface geometry was explicitly represented in the LES model based on very-high-resolution digital surface data. The WRF outputs are used as the basic flows in the LES.

Well-developed turbulent fluctuations from the basic flows were represented in the urban boundary layer over the LES domain. The observed ranges of wind fluctuations and gust factors were well reproduced in the LES. In addition, significant decelerations of wind speeds within the urban canopy layer were reasonably represented in the LES. The simulated features indicate that the present approach to couple an LES model with an NWP model should be useful in generating turbulent flows due to urban surface geometry under a real meteorological condition. Although the simulated meteorological fields in the present case did not largely vary during the simulated period, the present approach has an advantage in maintaining the simulated meteorological fields as the basic flow in the LES domain.

The smallest scale of WRF data is about 10 min because the WRF data at 1 min interval are quite similar to the observed 10 min winds, while the largest scale of LES is about 20 s, considering that the length of the driver domain is 1 km and the reference wind speed is about 40 m s^{-1}. Therefore, in order to fill this gap between the turbulence scales captured by the WRF and CFD models, we need to take a larger CFD domain which is sufficient to incorporate more variable meteorological influences.

Acknowledgements

We thank the two anonymous reviewers for their comments. This study is supported by grants from JSPS Scientific Research and the Inamori Foundation.

References

Chorin AJ. 1967. A numerical method for solving incompressible viscous flow problems. *Journal of Computational Physics* **2**: 12–26.

Golaz JC, Doyle JD, Wang S. 2009. One-way nested large-eddy simulation over the Askervein Hill. *Journal of Advances in Modeling Systems* **1**: 1–6.

Goldstein D, Handler R, Sirovich L. 1993. Modeling a no-slip flow boundary with an external force field. *Journal of Computational Physics* **105**: 354–366.

Gresho PM. 1992. Some interesting issues in incompressible fluid dynamics, both in the continuum and in numerical simulation. *Advances in Applied Mechanics* **28**: 45–140.

Janjic ZI. 2002. Nonsingular implementation of the Mellor-Yamada level 2.5 scheme in the NCEP Meso model. *NCEP Office Note* **437**: 61.

Kataoka H, Mizuno M. 2002. Numerical flow computation around aeroelastic 3D square cylinder using inflow turbulence. *Wind and Structures* **5**: 379–392.

Lund TS, Wu X, Squires KD. 1998. Generation of turbulent inflow data for spatially-developing boundary layer simulations. *Journal of Computational Physics* **140**: 233–258.

Mayor SD, Spalart PR, Tripoli GJ. 2002. Application of a perturbation recycling method in the large-eddy simulation of a mesoscale

convective internal boundary layer. *Journal of the Atmospheric Sciences* **59**: 2385–2395.

Nakayama H, Takemi T, Nagai H. 2011. LES analysis of the aerodynamic surface properties for turbulent flows over building arrays with various geometries. *Journal of Applied Meteorology and Climatology* **6**: 79–86.

Skamarock WC, Klemp JB, Dudhia J, Gill DO, Barker DM, Duda MG, Huang X-Y, Wang W, Powers JG. 2008. A description of the Advanced Research WRF Version 3, *NCAR Technical Note*, NCAR/TN-475+STR, 1.

Smagorinsky J. 1963. General circulation experiments with the primitive equations. *Monthly Weather Review* **91**: 99–164.

Xie Z-T. 2011. Modelling street-scale flow and dispersion in realistic winds towards coupling with mesoscale meteorological models. *Boundary-Layer Meteorology* **141**: 53–75, DOI: 10.1007/s10546-011-9629-x.

